

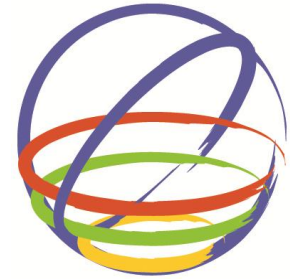
# Seismic Assessment of a Typical Masonry Residential Building in Bosnia and Herzegovina

**Naida Ademović**

*Senior Assistant, Faculty of Civil Engineering in Sarajevo, Bosnia and Herzegovina,*

**Daniel V. Oliveira**

*Associate Professor, ISISE, University of Minho, Depart. Civil Engineering, Portugal,*



**15 WCEE**  
LISBOA 2012

## **SUMMARY:**

The paper elaborates the seismic behaviour of a typical masonry building in B&H built in the 60's without any seismic guidelines. Numerical modelling has been done in two different software packages, namely DIANA and 3MURI. In both approaches, adequate constitutive assumptions were assumed to take into account the nonlinear behaviour of masonry.

Seismic vulnerability has been conducted by performing pushover and time history analyses. A comparison in terms of dynamic properties, crack pattern and capacity curves was done and a good agreement has been found between the two software packages. The paper's aim was to assess the seismic safety of this type of construction. A further objective was to investigate if simple software packages could be used for the assessment of these buildings. As a wide stock of this type of buildings is located through the former territory of ex-Yugoslavia, this work would enable a better understanding of this type of structures and quick overview of their actual seismic behavior.

*Keywords: masonry, nonlinear analysis, B&H residential masonry buildings, pushover, time-history analysis*

## **1. INTRODUCTION**

The paper discusses the behavior of a typical masonry building in Bosnia and Herzegovina built in the 60's and designed without any seismic guidelines, one of many similar structures spread throughout ex-Yugoslavia. As this kind of buildings represent a large portion building stock of residential unreinforced masonry buildings, which most probably do not satisfy the latest code provisions, this leads to the necessity for investigation of seismic vulnerability. The high seismic vulnerability of this type of building lies in its layout, having only load bearing walls in one direction. Moreover the vulnerability of these buildings is enhanced by its height (seven stories) and the fact that no seismic rules have been applied.

Two modeling approaches were followed. The first analysis was done by a Finite Element Method (FEM) utilizing the software package DIANA 9.4 (DIANA 9.4, 2009), and the second in 3MURI Program, which uses the Frame by Macro Elements (FME) method (S.T.A.-DATA, 2010) being one of the most practiced methods within this category available for the calculation of masonry structures, inspired by the "equivalent frame" method. In the paper it is clearly seen how sophisticated structural analysis can help and provide significant information regarding a better understanding of the structural behavior of these buildings. Additionally, calculations done with the simpler model are in a good correlation with the FEM calculations. It was able to "grasp" the damage pattern; not in the degree of DIANA calculations, but still quite good. On the basis of this it may be concluded that in this case calculation with 3MURI program could be recommended for future analysis of this type of structures, having quite good results with a less computation time. However, in the need for more precise information, the FEM approach should be utilized.

## 2. CASE STUDY

### 2.1 Description of the structure

The typical masonry building, see Figure 1 (a) and (b), is located in Sarajevo, in the part of the city called Grbavica. It is a seven level (basement + ground floor + 5 storeys) building. The plan view illustrated in Figure 2 shows the layout of the structure with load bearing walls in Y direction only. The structure has been design and built in 1957. During its time life there have been no changes regarding its layout and usage.

### 2.2 Geometry and materials

In the plan, the structure is of dimensions 38.0m by 13.0m with 7 levels. The structure is composed of load bearing walls only in the transverse direction (y direction, see also Figure 2) with slabs made of semi-prefabricated elements. The longitudinal walls are not considered as load-resisting elements as they have been made weak by many openings as shown in Figure 1 (b). The transversal bearing walls are brick masonry walls of 0.25m thick and a non-bearing façade wall made of hollow bricks of 0.125m thick, while the inner bearing walls are solid brick walls of 0.25m thick. Bricks are of standard dimensions 25x12x6.5cm, connected by cement mortar. The slabs are made out of "Herbst" concrete hollow elements as shown in Figure 3(a). The roof is of the same construction as the floors, providing continuity of the construction, and later on the possibility for additional storeys to be added. Construction of these blocks was regulated by Yugoslavian standards B.D1.030-1965 (Peulić, 2002). The basement walls are made out of concrete. Inner perpendicular walls are 0.38m thick, while the outer (longitudinal) walls are 0.30m thick, and two inner walls are 0.25m thick. As the span is larger than 3.0m it was foreseen, as per above mentioned standards at that time, to construct a transversal beam of 0.25m width with the same height as the slab, see Figure 3(b). Visual inspection revealed that there were no major damages on the structure.



**Figure 1.** Considered building, built in the year of 1957: (a) real structure; (b) East façade.

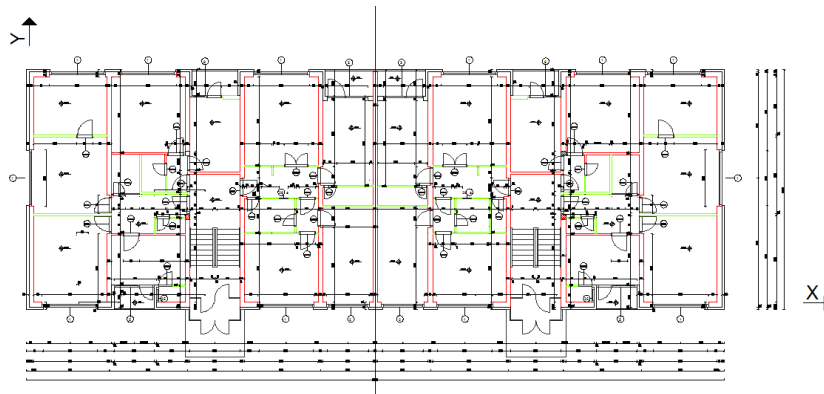


**Figure 2.** Plan of the floor and adopted axes system.

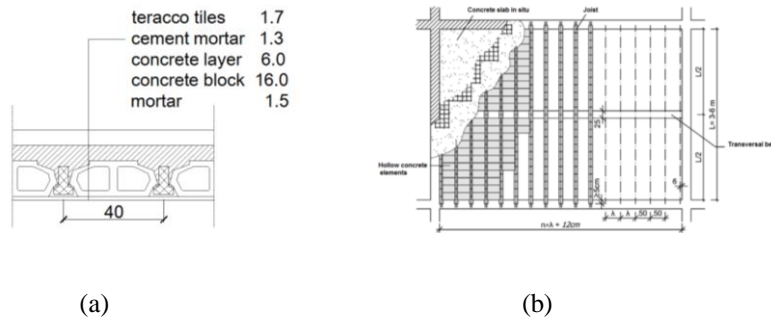


**Figure 3.** Constructive details: (a) Semi-prefabricated concrete elements; (b) Floor (Peulić, 2002).

### 3. NUMERICAL MODELS

As it has been seen from numerous examples, modeling of masonry structures is not an easy task (Lourenco, 2002). In this particular case, the main difficulties are attributed to the nonlinear behavior of masonry material and inadequate experimental information regarding mechanical properties of structural elements. The structure has been modeled resorting to two modeling strategies, as referred to in section 1. By the FEM an accurate geometrical and material modeling of the building can be obtained, however the computational time is very long. On the other hand, simplification regarding geometrical and material characteristics can be done in the equivalent frame approach. The following sections discuss the main features of both models.

In order to get all the necessary data regarding the geometry, structural details and state of the structure, preliminary in situ investigations have been conducted. Verification of the geometric data was done with laser distancemeters and total stations, on the basis of which AutoCAD drawings were performed as shown in Figure 1 (b) and Figure 2. In order to obtain data regarding the mechanical and physical properties of materials, laboratory experimental tests were done. Specifically, brick unit's compressive strength and compressive strength of concrete walls were determined.

#### 3.1 Description of the DIANA numerical model

The numerical model was made in DIANA 9.4 (DIANA 9.4, 2009) utilizing the geometrical data obtained from the original design as shown in Figure 4 (a). The structure was modeled by curved shell elements, corresponding to the quadrilateral element CQ40S type. This kind of element is characterized by 8 nodes and 5 degrees of freedom for each node (40 DOF per element). Rigid floors were assumed, enabling the distribution of the lateral loads to the walls in respect to their stiffness. After meshing, the final 3D numerical model consists of 84523 nodes and 28522 CQ40S elements, see Figure 4 (a).

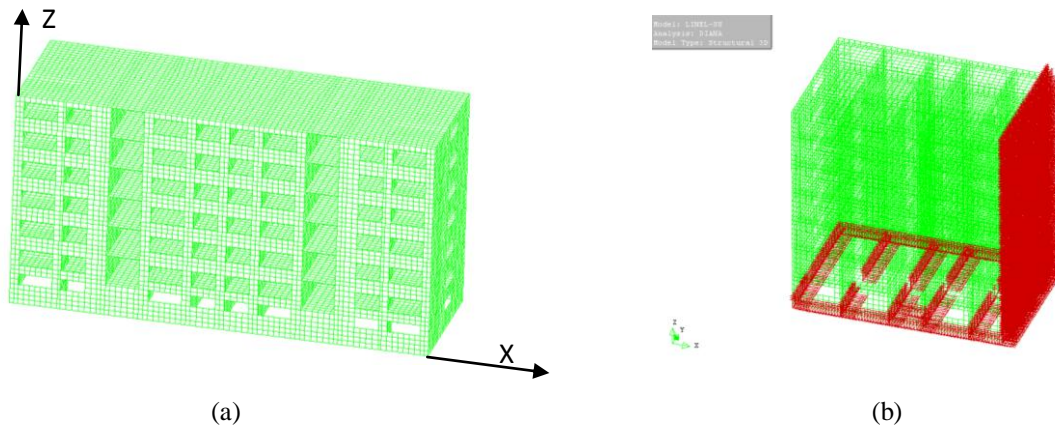


**Figure 4.** (a) Numerical model performed in DIANA and (b) Constrains for half of the model.

The mesh was kept the same for the static non-linear analysis and dynamic time history analysis, however due a very large number of elements and limited time, half of the structure was considered. This was enabled by the fact that the structure is symmetric. Adequate boundary conditions were used as shown in Figure 4(b).

Physical non-linear behavior of the masonry walls is defined through the adoption of the total strain fixed crack model, detailed in DIANA (DIANA 9.4, 2009). For hysteretic behavior of masonry a parabolic stress-strain relation for compression, based on Hill-type yield criterion, was chosen with no lateral confinement and no lateral crack reduction, see Figure 5. The tension path, based on Rankine-type yield criterion, was described by an exponential tension-softening diagram having a tensile strength of  $f_t = 0.2 \text{ N/mm}^2$  and a tensile fracture energy of  $G_f = 0.1 \text{ N/mm}$ . The post-cracked shear behavior was defined by taking into account the retention factor of its linear behavior, which reduces its shear capacity according to the following equation:

$$G^{cr} = \beta G$$

where  $\beta$  is the retention factor  $0 < \beta \leq 1$ , and  $G$  is the shear modulus of the uncracked material. The shear retention factor,  $\beta$ , was left at the default value of 0.01. This means that the shear strength of the material will be reduced to one percent of the original shear strength when cracks form. The material characteristics that have been utilized in the calculations are given in Table-1 for masonry and in Table-2 for concrete.

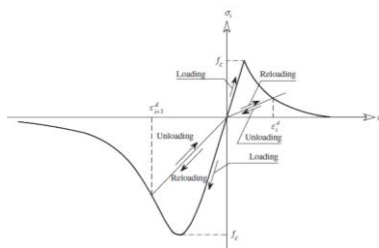


**Figure 5.** Hysteretic Behavior of Masonry (Mendes, et al., 2009).

**Table 1.** Masonry Data used as Input for Modeling.

Element	Thickness [m]	Compressive strength $f_k$ [N/mm <sup>2</sup> ]	Compressive fracture energy $G_{fc}$ [N/mm]	Tensile strength $f_t$ [N/mm <sup>2</sup> ]	Tensile fracture energy $G_f$ [N/mm]	E [N/mm <sup>2</sup> ] as per EC6	Poisson ratio $\nu$	Density $\rho$ [kg/m <sup>3</sup> ]
Façade walls	0.375	4.07	6.51	0.20	0.10	4070	0.20	2700*
Inner walls	0.25							1900

**Table 2.** Concrete Data used as Input for Modeling.

Element	Thickness [m]	Mean comp. strength $f_{cm}$ [N/mm <sup>2</sup> ]	Mean tensile strength $f_{ctm}$ [N/mm <sup>2</sup> ]	E [N/mm <sup>2</sup> ]	Poisson ratio $\nu$	Density $\rho$ [kg/m <sup>3</sup> ]
Floor	0.265	24	2.2	30000	0.20	2190
Roof	0.435					2050
Walls	0.380					2400

For the chosen CQ40S quadrilateral elements, the in-plane Gauss integration scheme was selected with 3x3 integration points on the sides, minimum as per (Zienkiewicz, 2005), while thought the thickness in order to capture the non-linear behavior 5 points were selected, and this is defined by the Simpson rule. As the structure is large, one of the things that had to be kept in mind was the computation time, so that was an additional parameter to be taken into account for the choice of the integration points. The Regular Newton-Raphson method was chosen as the iteration method with arc-length control. Model of energy convergence was adapted for this model with the tolerance of 1.0E-03.

### 3.2 Description of the 3MURI numerical model

The structure was modeled in 3MURI having the same material and geometrical characteristics as defined before. The model consists of 7 levels, 218 - 3D nodes, 34 - 2D nodes, and 506 elements. The view of the structure and elements is presented in Figure 6.



**Figure 6.** View of the structure and its elements in 3MURI.

### 3.3 Comparison of dynamic characteristics

Eigen-frequencies and eigen-modes were compared as well as the mass participation factors in the first three modes as presented in Table 3. As it can be seen from Table 3, the maximum difference for the first three modes is 19.2% while for mass participation is 9.2%. The mode shapes obtained by both models have the same configuration. Therefore, it can be concluded that a good correlation between the two calculations has been obtained.

**Table 3.** Comparison of periods and eigen-frequencies (DIANA vs. 3MURI).

Mode	Period T [s]		Difference [%]	Mass participation M [%]		Difference [%]
	DIANA	3MURI		DIANA	3MURI	
1 <sup>st</sup>	0.46	0.51	10.9	67.33 (x)	73.31 (x)	8.9
2 <sup>nd</sup>	0.26	0.31	19.2	67.39 (x)	73.56 (x)	9.2
3 <sup>rd</sup>	0.25	0.28	12.0	58.79 (y)	62.96 (y)	7.1

## 4. PUSHOVER ANALYSIS

### 4.1 Results obtained with DIANA

The analysis of the seismic behavior has been conducted by the application of a non-linear static analysis (Pushover), a performance-based methodology, based on an incremental increase of a pre-defined horizontal force distribution on a structure and constant gravity loads. Results from the pushover analysis are usually assumed as a result envelope of all the responses derived from the non-linear dynamic analysis. The structure was exposed only to the horizontal forces in the " $\pm Y$ " direction, as shown in Figure 7 as it would not be able to resist earthquakes acting along the " $\pm X$ " direction (weaker direction of the building). The horizontal load was applied in a stepwise fashion proportional to mass distribution. A control node was chosen in the line of symmetry at the roof level, node no. 44014, as shown in Figure 7. Two additional nodes in the same line were selected (node 44035 and 43935) in order to verify the behavior of the slab.

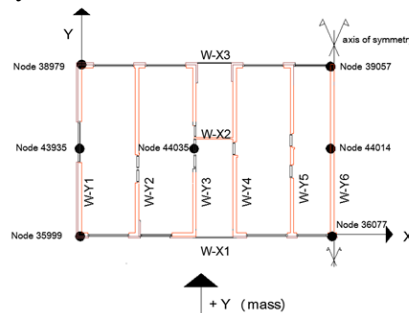


**Figure 7.** Location of the nodes; wall labeling; and direction of the horizontal force.

Figure 8 shows the capacity curve for "+Y" direction. The nonlinear behavior of the structure starts very early and the maximum load coefficient reached is of  $\alpha=0.518$ . It is also possible to observe that



the movement of the nodes at the top of the structure in the same horizontal line (nodes 43935, 44035 and 44014) as shown in Figure 8 proved the rigid floor assumption adopted in section 3.

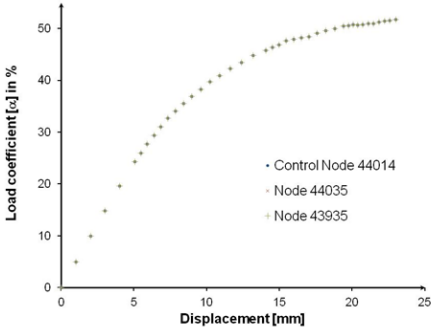


**Figure 8.** Capacity Curves for Nodes 44014, 44055 and 43935.

At the final stage of loading ( $\alpha=0.518$ ), the largest amount of cracks is located at the walls W-Y6 and W-Y5(see Figure 9). Shear damage of transversal walls (parallel to the Y direction) is evident, which would further on lead to shear failure. Additionally, due to bending above the openings, bending damage and maybe later on even failure is to be expected in these locations. This has implications on the development of the cracks on the facade wall W-X1 and W-X3, but to a smaller extent, where evident compression (seen from the principal compressive stresses, not presented here) damage and even failure at the ground level is noticed, with most probably later on local falling out of masonry. The appearance of the cracks at the last loading step (equivalent to 51.8% of the force) for walls W-Y4, W-Y6 and W-X1 is shown in Figure 9.

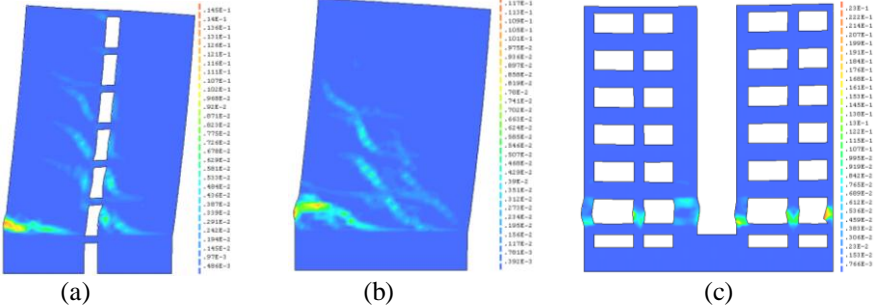


**Figure 9.** Principal tensile strains for  $\alpha=0.518$ : (a) W-Y4; (b) W-Y6; (c) façade wall W-X1.

This kind of damage was observed on a structure of a similar type after the earthquake that struck Skopje in 1963, as shown in Figure 10. The concentration of damage is located on the ground floor with diagonal cracks between the openings probably caused by shear. Falling of the masonry in one of the corners is evident.



**Figure 10.** Concentrated damage at the ground floor (Petrovski, 2003).

In both directions the structure is able to sustain a force in the value of 45% to 52% of its weight (Figure 11), which could be connected to the rather good characteristics of masonry. Some redistribution of the forces might have been caused due the existence of the longitudinal wall (W-X2).

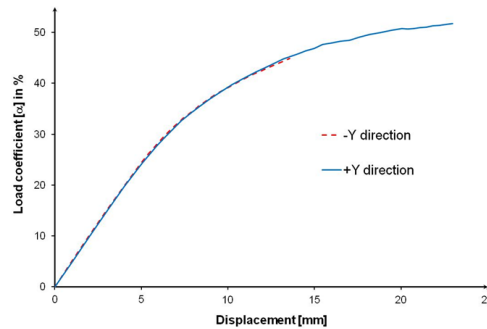


**Figure 11.** Comparison of Capacity Curves for "+Y" and "-Y" direction for control node 44014.

## 4.2 Results obtained with 3MURI

### 4.2.1 Results obtained in the "+Y" direction

The capacity curve of the structure while exposed to the load patten proportional to the mass in "+Y" direction is shown Figure 12. As it can be seen from Figure 13 (see also Figure 16(c)) bending damage is located at the spandrels above the doors and windows, and even in some of the walls bending failure is observed. Shear damage is seen on all the perpendicular walls (Y direction) and especially on the wall W-Y6. The basement which is made out of concrete remains undamaged during the application of the load.

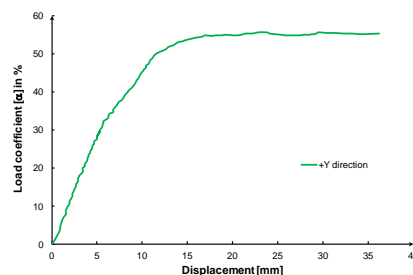


**Figure 12.** Capacity curve for "+Y" direction.



**Figure 13.** Damage in the walls in "+Y" direction at the failure stage: (a) W-Y4; (b) W-Y6; (c) W-X1; (d) legend.

### 4.2.2 Results obtained in the "+X" direction

In order to verify the assumption of the weakness of the structure in the X-direction the structure was subjected additionally to a pushover analysis in the " $\pm$  X" direction, following the same procedure as applied to the " $\pm$  Y" direction. Figure 14 shows that the structure possesses a very limited resistance along the " $\pm$  X", as assumed initially in this study. The structure experiences the first crack already at

4.5% of the force, where as the maximum coefficient reached amounts to only 9%. Failure of the façade walls is due to bending and compression forces at the ground level, as illustrated in Figure 15 and Figure 16.

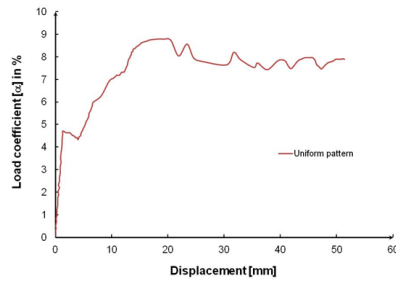


Figure 14. Capacity curve for "+X" direction.

No.	Insert in report	Earthquake	Uniform pattern of lateral load	Ecc. [cm]	Dmax ULS [mm]	Du ULS [mm]	q* ULS	Dmax DLS [mm]	Dd DLS [mm]	Alpha u	Alpha e
1	<input type="checkbox"/>	+X	Masses	0,00	42,39	51,39	4,206	21,19	20,67	0,713	0,975
2	<input type="checkbox"/>	+X	First mode	0,00	25,77	64,00	6,945	12,40	6,88	0,432	0,587
3	<input type="checkbox"/>	-X	Masses	0,00	20,16	51,34	5,321	9,28	40,15	0,564	3,837
4	<input type="checkbox"/>	-X	First mode	0,00	25,63	62,53	6,901	12,32	6,86	0,435	0,589

Colour legend

- Satisfied
- Not satisfied
- Self weight not converging

Figure 15. Results in "±X" direction

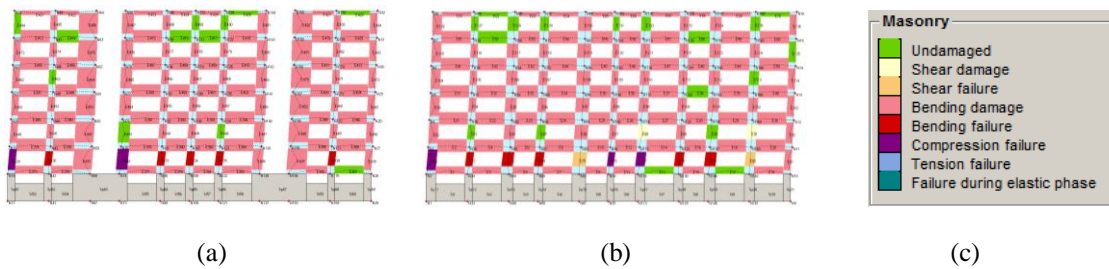


Figure 16. Damage in the façade walls in "+X" direction: (a) wall W-X1; (b) wall W-X3; (c) legend.

#### 4.3 Comparison of pushover curves

The capacity curves for the "+Y" direction obtained by DIANA and 3MURI are compared in Figure 17. The capacity curve achieved using DIANA, once the maximum strength was obtained, stopped due to convergence issues. The capacity curve obtained from 3MURI after reaching the maximum strength continues on with a horizontal plateau, as it adopts elastic-ideal plastic constitutive curves for the structural elements. The difference in the stiffness can be attributed to the rigid connection between spandrel and pier elements assumed by 3MURI. The difference regarding the maximum load coefficient is about maximum 6.9%, which can be declared as acceptable given the differences between the modeling strategies.

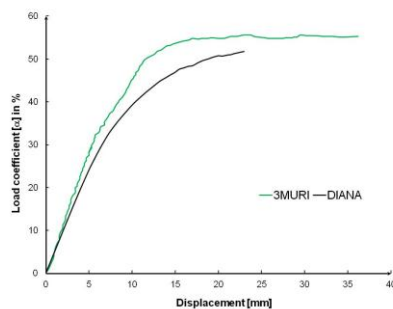


Figure 17. Capacity Curves: DIANA vs. 3MURI in "+Y" direction.



## 5. TIME HISTORY ANALYSIS

The structure was exposed to the Petrovac short-period earthquake, recorded during the earthquake at Petrovac on the April 15, 1979, (Montenegro), in order to analyze the response of the structure. The ground motion record was previously filtered and scaled using Seismosignal software (Seismosignal, 2010) to obtain a peak ground acceleration (PGA) of 0.10g and then applied in the Y direction of the building as this corresponds to the Sarajevo region. The differences in the soil conditions between Sarajevo and Petrovac were not taken into account.

### 5.1 Results of the analysis

The maximum displacement is observed at the last floor in the value of 11.38mm at the time  $t_3=7.65s$  and the respective damage pattern is shown in Figure 18. It is interesting to note that the maximum drift in floors 1, 2 and 4 is reached at the same time instance, whereas floors 5 and 6 reach their maximum drift at the same time. The biggest jump in the inter-storey drift is observed at the ground level, at the height of 2.8m, being equivalent to 0.51%. The cause of damage in walls is a high value of the drift (which is a "jump" between floors). The jump in the drift values is a sign of deep change in stiffness. The envelope shows the largest storey drift is 0.78% located at the second floor (8.4m), which is consistent to the damage pattern shown before. The large drift imposes severe deformation and ductility demand at locations of the lower floors. Additionally, hysteresis curve has been determined for the control node 44014. The maximum load coefficient of 0.23 was reached while the maximum displacement was 11.38mm.

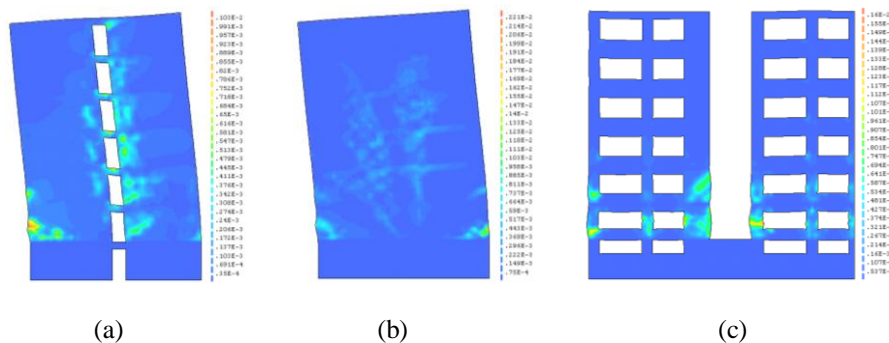


**Figure 18.** Damage of the walls at  $t_3=7.79s$ : (a) W-Y4; (b) W-Y6; (c) W-X1.

On the basis of the results obtained from the THA it can be seen that the structure has a typical shear behavior. The walls parallel to the load direction experience diagonal cracks caused by shear, and due to the cyclic loading, an evident diagonal "X" type cracks are formed. At the location of the openings the concentration of damage is evident due to stress concentrations. The major concentration of the damage is located between the basement and the ground floor, which can be connected with the discontinuity and large difference of the stiffness. Large damage is observed in the lower floors where the largest inter-story drift was observed, imposing severe deformation and ductility demand at these. This kind of behavior has been identified by the previous earthquakes on a similar structure in Skopje and by experiments conducted by Tomažević in Slovenia. The propagation of the damage slowly expands to the upper floors on the façade walls. The earthquake action, as a cyclic loading causes the degradation of the stiffness of the structure.

## 6. CONCLUSIONS

Several comparisons resorting to different modeling strategies and analysis techniques have been made, and it can be concluded that the choice regarding the level of sophistication of the model has an impact on the accuracy of the results as well as on the degree of detail regarding the representation of the crack pattern. The frequencies and mode shapes obtained by both modes are quite similar. It can be concluded that a good correlation between the two calculations has been obtained. Additionally, when

looking at general behavior of the structure regarding the crack development and failure mechanism, it can be seen that the two models are consistent in the application of the pushover method and even the THA in DIANA. The global view of damage is visible as well as the propagation of a certain mechanism failure in 3MURI program, while DIANA gives a more detailed crack pattern with a clear manifestation of stiffness degradation, and localization of the cracks and damage in the structure. The DIANA model gives a very detailed crack pattern, however at the same time the computational time is much longer in respect to 3MURI. The regularity of the structure has also implications as the results obtained with 3MURI (simpler model) are in a very good correlation with the results obtained by DIANA.

In both calculations the structure showed a typical shear failure mode in the walls parallel to the load direction. In the façade walls (along the x-axis) the concentration of damage in both models is seen at the lower floors with a slow propagation over the height of the structure. The location of this concentrated damage can be connected to the large stiffness change at this location.

The structure showed a "satisfactory" behavior in the "±Y" direction, passing the verifications defined by Eurocode 8 in the 3MURI program, however the structure failed in the "±X" direction implying that globally the structure is not safe. This leads to the necessity of strengthening the structure with adequate measures (Ademović, 2011).

## REFERENCES

- Ademović, N. (2011). Structural and Seismic Behavior of Typical Masonry Buildings from Bosnia and Herzegovina. *Advanced Masters in Structural Analysis of Monuments and Historical Constructions*. University of Minho, Portugal.
- Anderson, D. and Brzev, S. (2009). Seismic Design Guide for Masonry Buildings. *Canadian Concrete Masonry Producers Association*. (Report). Toronto, Canada
- Cattari, S. and Lagomarsino, S. (2008). A strength criterion for the flexural behaviour of spandrel in unreinforced masonry walls. *Fourteenth World Conference on Earthquake Engineering*. Beijing, China.
- CEN Eurocode 8. (2003). Design of Structures for Earthquake Resistance, Part 1: General rules, seismic action, and rules for buildings. prEN 1998-1-1. *European Committee for Standardization, Management Centre in Brussels*. Brussels.
- Chopra, A. (2007). Dynamics of Structures, Pearson Prentice Hall, New Jersey.
- DIANA 9.4. (2009). TNO Displacement method ANALYSER 9.4-Finite element analysis. *User's Manual*, release 9.4. Netherlands.
- Drysdale, R. G., Hamid, A. A. and Baker, L. R. (1999). Masonry Structures: Behaviour and Design, The Masonry Society, Boulder, Colorado, Second Edition.
- Flores, L.E. and Alcocer, S.M. (1996). Calculated Response of Confined Masonry Structures. *Eleventh World Conference on Earthquake Engineering*. Elsevier Science Ltd.
- Lourenco, P.B. (2002). Computations of historical masonry constructions. *Prog Struct Eng Master*. **4(3)**, 301-319.
- Mendes, N. and Lourenco, P. B. (2009). Seismic Assessment of Masonry "Gaioleiro" Building in Lisbon, Portugal *Journal of Earthquake Engineering*.
- Petrovski, T.J. (2003). Damaging Effects of July 26, 1963 Skopje Earthquake. *International Conference 40 years 1963 Skopje Earthquake*, European Earthquake Engineering (SE-40EEE), Skopje
- Peulić, Đ. (2002). Konstruktivni elementi zgrada, Croatiaknjiga, Zagreb.
- S.T.A.-DATA 3 Muri. (2010). Manual, STA DATA srl, Torino.
- Seismosignal Earthquake Engineering Software Solutions. (2010), Version 4.2.1.
- Tomažević, M. Bosiljkov, V. and Weiss, P. (2004) Structural Behavior Factor for Masonry Structures. *13th World Conference on Earthquake Engineering*. Vancouver. **Vol, paper 2642**.
- Tomažević, M. (1987). Dynamic Modelling of Masonry Buildings: Storey Mechanism Model as a Simple Alternative. *Earthquake Engineering and Structural Dynamics*. **Vol 15**, 731-749.
- Tomažević, M. (1999). Earthquake-Resistant Design of Masonry Building, Imperial College Press, Tom. I. London.
- Tomažević, M. and Klemenc, I. (1997). Verification of Seismic Resistance of Confined Masonry Buildings. *Earthquake Engineering and Structural Dynamics*. **Vol. 26**, 1073-1088.
- Tomažević, M. and Weiss, P. Seismic Behavior of Masonry Buildings. (1991). Reinforced versus Unreinforced Masonry *9th International Brick/Block Masonry Conference*, Berlin. **Vol. 1**, 552-559.
- Zienkiewicz CBE, FRS. (2005). The Finite Element Method: Its Basis and Fundamentals, Elsevier, Barcelona.